Pergamon

Int. J. Solids Structures Vol. 35, Nos 34–35, pp. 4963–4979, 1998

Printed in Great Britain
0020-7683/98/$—see front matter

PII: S0020-7683(98)00104-8

A METHOD FOR THE DETERMINATION OF MECHANICAL PARAMETERS IN A POROUS ELASTICALLY DEFORMABLE MEDIUM: APPLICATIONS TO BIOLOGICAL SOFT TISSUES

S. NAILI,† C. ODDOU and D. GEIGER
Laboratoire de Mécanique Physique, Université Paris XII Val-de-Marne, Faculté des Sciences et Technologie, CNRS UPRES-A7052, 61 Avenue du Général de Gaulle, 94010 Créteil Cédex, France

(*Received* 18 *June* 1997; *in revised form* 5 *February* 1998)

Abstract—A further approach has been tentatively envisaged for the determination of the mechanical parameters characterizing the unsteady behaviour of soft biological tissues considered as porous, elastically deformable media, saturated with a viscous fluid. If the two solid and fluid phases are incompressible, the parameters to be determined are: the drained Young's modulus and Poisson's ratio, the permeability of the porous solid structure and the dynamic viscosity of the interstitial fluid.

Standard ramp–relaxation tests have been performed in order to investigate the time evolution of the force acting upon tissular discoïdal samples subjected to unconfined compressive strains, under controlled environmental conditions. For moderate compressive strains, such a response in resultant force, characterizing a stress diffusion phenomenon within the medium, can be analyzed using a spectral decomposition with orthogonal eigenvectors. Such an analysis reveals that the overall response is defined by its asymptotic behaviour during both compression and relaxation phases, leading to the evaluation of the Young's modulus and Poisson's ratio. Moreover, the determination of the relaxation time leads to the evaluation of the specific permeability of the structure—the dynamic viscosity of the fluid being already known.

A few examples of experimental tests data, involving both rubber foam, myocardium tissue in passive state and fibroblastic biological collagenic gels, are presented here in order to illustrate and validate such a rheological methodology. Particular attention is paid to the relations between the poroelastic behaviour and microstructural parameters of the material, with an emphasis on possible nonlinear effects arising from these very deformable media.

1. INTRODUCTION

From structural and mechanical standpoints, soft tissues and soils turn out to be very similar. In this context, we have developed an original method for the determination of mechanical parameters characterizing a porous elastically deformable medium, saturated by a Newtonian fluid, in which each phase—structure and fluid—is incompressible.

Biot (1941) formulated the basic theory of the deformation of a porous, isotropic, elastic solid, saturated by a Newtonian fluid and which is subjected to small strains. If each phase—structure and fluid—is considered as incompressible, this theory requires the knowledge of four mechanical parameters—drained Young's modulus, drained Poisson's ratio, permeability of the structure, and dynamic viscosity of the interstitial fluid—the terminology of Rice and Cleary (1976) being used. There are two main approaches for the determination of the mechanical parameters of a porous elastic solid saturated by a viscous fluid: (i) measurement of the radial displacement under 1-D axial tension with no variation of the fluid content (e.g. see Coussy, 1991); (ii) measurement of the velocity of acoustic waves in the sample (e.g. see Bourbié *et al.*, 1987), following the work of Biot (1946).

As far as biological tissues are concerned, many studies have corroborated on unsteady rheological properties of articular cartilage (e.g. see Mow *et al.*, 1980). Such properties have been analyzed from both standpoints: the thermodynamics of mixtures and two

† Author to whom correspondence should be addressed. Tel.: +33 1 45 17 14 45. Fax: +33 1 45 17 14 33. E-mail: naili@univ-paris12.fr

scales analyses of the constitutive mechanical equations—our experimental studies mostly concerning the case of uniaxial unconfined compression. The frictional drag due to the relative motion of the two phases was shown to be the most important factor governing the fluid–solid rheological properties of the tissue under unsteady compression, although the organic fibrous polymeric matrix could be intrinsically viscoelastic (e.g. see Mak *et al.*, 1986). In those permeable and soft hydrated biological tissues, the finite deformation of the solid matrix, on the one hand, and strain dependent permeability effects, on the other, can lead to nonlinear behaviour (e.g. see Mow *et al.*, 1986; Yang and Taber, 1991).

In the present work, we concentrate on the case in which the constituents are separately incompressible. A simple method is proposed for the determination of the drained Young's modulus and the drained Poisson's ratio, the permeability of the structure and the dynamic viscosity of the fluid being determined as usual (e.g. see Bourbié *et al.*, 1987). A standard unconfined compression test was conducted in order to investigate the asymptotic behaviour of discoïdal samples of tissues subjected to controlled small compression at a constant strain rate followed by a long period of relaxation. The time variation of the overall macroscopic deformation being given at the scale of the sample, the method further imposes an analytical determination of the compression and relaxation resultant force acting upon the medium. For this purpose, this resultant force was determined by using spectral decomposition with orthogonal eigenvectors, following the work of Mandel (1953). The analysis of the time evolution of such a force—particularly its asymptotic behaviour during compression—shows that the ordinate at the origin is a measure of the drained Poisson's ratio while the slope of the curve yields the drained Young's modulus. Thereby, measuring the radial displacement is unnecessary and the variation of fluid content is irrelevant (e.g. see Le Gallo *et al.*, 1991; Naili *et al.*, 1994). With the usual methods implying the steadiness of the amount of overall fluid content, the measurement of the radial displacement is indeed difficult to carry out when dealing with soft materials like rubber foam or biological materials. Djerad *et al.* (1992) have used partly this new method for the determination of mechanical parameters in the cardiac muscle. An analysis of experimental data obtained during compression and relaxation tests on pig heart cylindrical wall samples were correctly interpreted by using this approach.

This paper falls into five main sections. The second section deals mainly with the mathematical formulation of the mechanical behaviour of a porous elastically deformable medium saturated by a Newtonian fluid, under unsteady small strains conditions. Section 3 itself falls into two parts; the first one describes the theoretical model with these hypotheses and conditions, while the second gives an analytical solution of the theoretical model. In particular, we obtain the resultant force during compression and relaxation tests by using spectral decomposition with orthogonal eigenvectors. In Section 4, we analyze theoretical results. Section 5 illustrates the method as applied to rubber foam sample, myocardium tissue in passive state and fibroblastic biological collagenic gels, as currently experimentally studied in our laboratory.

2. BEHAVIOUR OF A POROUS ELASTICALLY DEFORMABLE MEDIUM

We consider the quasistatic behaviour of an isotropic, porous, elastically deformable medium with constant porosity, saturated by a Newtonian fluid. If the constituents are separately incompressible, and the structure only subjected to a small strain, the constitutive equations are given by:

$$\boldsymbol{\sigma} = \frac{E}{(1+v)}\boldsymbol{\varepsilon} + \frac{Ev}{(1+v)(1-2v)}\{\mathrm{Tra}\,\boldsymbol{\varepsilon}\}\mathbf{I} - p\mathbf{I}, \tag{1}$$

$$\theta = \mathrm{Tra}\,\boldsymbol{\varepsilon} \tag{2}$$

where $\boldsymbol{\varepsilon}$ denotes the symmetrical strain tensor for small strains, $\boldsymbol{\sigma}$ the symmetrical tensor of total stress, p the pore fluid pressure, θ the variation of the relative fluid content of the

structure, E its drained Young's modulus and ν its drained Poisson's ratio. Tra and **I** designate the trace and the identity operators, respectively.

By writing the equilibrium equation of the structure, we obtain the following system of displacement and pressure coupled equations:

$$\frac{E}{2(1+\nu)}\left[\Delta \mathbf{U}+\frac{1}{1-2\nu}\mathbf{Grad}(\mathrm{Div}\,\mathbf{U})\right]-\mathbf{Grad}\,p=\mathbf{0}, \tag{3}$$

$$\frac{\partial}{\partial t}(\mathrm{Div}\,\mathbf{U})=\frac{\kappa}{\mu}\Delta p, \tag{4}$$

where **U** denotes the structure displacement vector, κ the permeability of the structure, μ the dynamic viscosity of the fluid, Δ, **Grad** and Div designate the Laplacian, gradient and divergence operators, respectively.

These equations were obtained by combining Darcy's law with the mass conservation equation for the fluid, ignoring the body force per unit mass and inertia force, and assuming that the scalar, vector and tensor fields are "smooth" enough to allow a mathematical differentiation of those fields in space and time.

By taking the divergence of eqn (3) and by combining it with eqn (4), we obtain the consolidation equation, given by:

$$\frac{\partial \theta}{\partial t}=c\Delta\theta, \tag{5}$$

where c is the consolidation coefficient:

$$c=\frac{E(1-\nu)}{(1+\nu)(1-2\nu)}\frac{\kappa}{\mu}. \tag{6}$$

A dimensional analysis of the diffusion eqn (5) reveals a characteristic time τ, the so-called consolidation time, given by:

$$\tau=\frac{a^2}{c}=\frac{\mu a^2}{E\kappa}\frac{(1+\nu)(1-2\nu)}{(1-\nu)}, \tag{7}$$

where a is a typical length of the tested medium.

3. METHODS

3.1. *Theoretical model: hypotheses and conditions*

Consider a thin plug of tissue—denoted by Ω—lying on the impermeable rigid and perfectly smooth flat base of a tank base filled with an incompressible Newtonian fluid. Such a porous sample, whose height and radius are, respectively, denoted as h and a, is initially saturated with the same fluid. It is loaded along its **z** axis, via an impermeable and perfectly smooth moving upper plate, its lateral surface being unconfined and permeable.

Changes in the structure geometry are described in cylindrical coordinates. Taking in to account the axial symmetry of the medium the problem is then twofold. The variables will be denoted as r and z, and the local basis $(\mathbf{e}_r, \mathbf{e}_\theta, \mathbf{e}_z)$ in cylindrical coordinates will be used. The boundary conditions can be written as follows:

- at $r = a$, the pressure being assumed to be zero, and the surrounding fluid being at rest, there is no radial stress: $p = 0$ and $\boldsymbol{\sigma}\mathbf{n} = \mathbf{0}$ for all $t > 0$, where **n** is the outer normal unit vector along the boundary $r = a$,
- at $z = 0$ and h, "the boundaries are impermeable": $\partial p/\partial z = 0$, for all $t > 0$.

To these boundary conditions, the initial condition at $t = 0$ must be added: Div $\mathbf{U} = 0$, for all point M in Ω.

The kinematic boundary conditions for this compression and relaxation test imply that in the first step, during a finite duration t_0, the sample is subjected to a compression at constant macroscopic strain rate v. In the second step, the sample relaxes under a constant strain. For each step, the displacements of the base surfaces of the sample are given by:

— at $z = 0$, the vertical displacement is zero: $\mathbf{U}\cdot\mathbf{z} = 0$, for all $t > 0$,
— at $z = h$, the displacement is imposed and is considered to be small in comparison with h:

$$\mathbf{U}\cdot\mathbf{z} = -vt, \quad \forall t \in [0, t_0], \quad \text{and} \quad \mathbf{U}\cdot\mathbf{z} = 0, \quad \forall t > t_0.$$

These conditions only obtainable if the contacts between the tested sample and the containing tank and upper plate, as previously defined, are perfectly frictionless. These are important assumptions that will be justified by experimental analysis. Indeed, boundary friction may have a significant influence on an unconfined compression response, especially for samples with a small thickness–diameter aspect ratio. Analytical (e.g. see Kim *et al.*, 1995) and numerical (e.g. see Spilker *et al.*, 1990) solutions have been developed to address plate friction.

Due to both sample geometry and adopted loading mode, we assume that, for small strains, the displacement vector $\mathbf{U}$ can be written as:

$$\mathbf{U} = U_r(r, t)\mathbf{e}_r + U_z(z, t)\mathbf{e}_z, \tag{8}$$

where U_r and U_z are the components of the displacement in the local basis.

In addition, we shall assume that both strain and pressure do not depend on z. Therefore, the stress tensor $\boldsymbol{\sigma}$ is only a function of r and t.

3.2. *Analytical solution of the theoretical model*

An identical analysis was published by Armstrong *et al.* (1994). However, these authors offered a solution equivalent to ours for the resultant of the compression–relaxation stress but in terms of Laplace transforms. The difficulty of their method resides in the calculation of the inverse Laplace transforms. Thus, the explicit solutions for all r are not given for the displacement and the fluid pressure.

Our analytical solution of the problem is based upon the same method as the one worked out in Cartesian geometry by Naili *et al.* (1992). The solution can thus be written as:

$$U_r(r, t) = \sum_{k=0}^{\infty} A_k \frac{1}{\omega} J_0(\omega_k r)\cdot e^{-s_k t} + v\frac{v}{h}rt - \frac{(1-2\nu)}{16c}\frac{v}{h}r^3 + \frac{(1-2\nu)(3-2\nu)}{16hc}va^2 r, \tag{9}$$

$$U_z(z, t) = -vt\frac{z}{h}, \tag{10}$$

$$p(r, t) = \frac{\mu}{4\kappa}(1-2\nu)\frac{v}{h}(a^2 - r^2) + \frac{\mu}{\kappa}c\sum_{k=0}^{\infty} A_k(J_0(\omega_k r) - J_0(\omega_k a))\cdot e^{-s_k t}, \tag{11}$$

where J_m is the Bessel function of first kind of order m, s a constant defined by $s = c\omega^2$.

The value of A_k is given by the relation:

$$A_k = \frac{(1-2\nu)v}{ch\omega_k^2}\frac{\omega_k a J_0(\omega_k a) - 2J_1(\omega_k a)}{\omega_k a[J_0^2(\omega_k a) + J_1^2(\omega_k a)] - 2J_0(\omega_k a)J_1(\omega_k a)}, \tag{12}$$

and w_k results of the following characteristic equation:

$$\omega a(1-\nu)J_0(\omega a) = (1-2\nu)J_1(\omega a). \tag{13}$$

The number of distinct and strictly positive roots of eqn (13) is infinite.

Now, by using the constitutive equation described by eqn (1), the compression stress is given by:

$$\sigma_{zz} = -E\frac{vt}{h} - (1-2\nu)\frac{v}{h}\frac{\mu}{4\kappa}\left[\frac{(2\nu-1)}{(1-\nu)}r^2 + \frac{2(1-\nu)-\nu(3-2\nu)}{2(1-\nu)}a^2\right] - \frac{\mu c}{\kappa}\sum_{k=0}^{\infty} A_k\left[\frac{(1-2\nu)}{(1-\nu)}J_0(\omega_k r) - J_0(\omega_k a)\right]\cdot e^{-s_k t}. \tag{14}$$

The resultant of the compression stress at $z = 0$ is obtained by evaluating the following integral:

$$F(t) = \int_{S_0} \sigma_{zz}\, \mathrm{d}S,$$

where S_0 is the cross-section of the sample at $z = 0$. By using the characteristic eqn (13), this integral leads to:

$$F(t) = \pi a^2 E\frac{v}{h}t + (1-2\nu)^2 F_0\left[\frac{1}{8} - \sum_{k=0}^{\infty}\frac{\mathrm{e}^{-s_k t}}{\{(1-\nu)^2(\omega_k a)^2 - (1-2\nu)\}(\omega_k a)^2}\right],$$
$$\forall t \in [0, t_0] \tag{15}$$

where $F_0 = \pi a^4(v/h)(\mu/\kappa)$.

The relaxation phase is studied by imposing $\varepsilon_{zz} = -vt_0/h$, for all $t \geqslant t_0$. The continuity of the fields, especially the continuity of the relative fluid content variation θ, gives the initial condition at $t = t_0$. This condition corresponds to the transition from the compression to the relaxation phases.

The stresses during relaxation are determined after some algebra, as follows:

$$\sigma_{zz} = -E\frac{v}{h}t_0 - \frac{\mu c}{\kappa}\sum_{k=0}^{\infty} B_k\left[\frac{(1-2\nu)}{(1-\nu)}J_0(\omega_k r) - J_0(\omega_k a)\right]\cdot \mathrm{e}^{-s_k t}, \tag{16}$$

where B_k is given by: $B_k = A_k(1-e^{s_k t_0})$, and ω_k is root of eqn (13).

And finally, the resultant of the relaxation stress at $z = 0$ is given by:

$$F(t) = \pi a^2 E\frac{v}{h}t_0 + (1-2\nu)^2 F_0\left[\sum_{k=0}^{\infty} B_k\,\mathrm{e}^{-s_k t}\right], \quad \forall t \geqslant t_0. \tag{17}$$

4. ANALYSIS OF THE THEORETICAL RESULTS

After a period of time sufficiently "larger" than the consolidation time τ, as defined by eqn (7), the force given by eqn (15) is reduced to the following simplified expression:

$$F(t) = \pi a^2 E\frac{v}{h}t + (1-2\nu)^2 F_0. \tag{18}$$

From a practical point of view, we will show in Section 5 how to obtain the order of magnitude of the consolidation time τ.

This is the equation of a straight line whose ordinate at the origin enables us to measure ν, if μ and κ have been previously otherwise determined, and whose slope gives E. Therefore,

during the ramp phase of the compression test, we have only to record the time evolution of the resultant force. This method has the advantage of enabling the measurement of the drained Poisson's ratio value without having to determine the radial displacement. However, it actually requires accurate measurements of the permeability κ of the structure, in order to obtain a good estimation of the drained Poisson's ratio ν.

Furthermore, force measurements during the relaxation phase allow to verify the measurement of drained Young's modulus because the asymptotic behaviour of the resultant force during the relaxation, as given by eqn (17), also yields the value of this parameter. Indeed, when time tends to infinity, the eqn (17) is reduced to the following simplified expression:

$$F(t) = \pi a^2 E \frac{v}{h} t_0. \tag{19}$$

It is worth noting that, in this approach, the transient steps which appear at both the beginning of the ramp and the relaxation phases are not used in order to characterize the medium. The measured properties are derived from the steady-state asymptotic behaviour of the structure during either the ramp or the relaxation phases of the test, assuming the medium to behave as a poroelastic medium. Nevertheless, as a method of validation, the resultant force during compression as predicted by the model when using these values for ν and E in eqn (18), must be checked against the resultant force measured throughout the transient phase.

Moreover, such measurements need a sufficiently long time which could be incompatible with the assumption of a final small strain.

Furthermore, a negative value of the drained Poisson's ratio can be surprising, but this result stands within the allowed theoretical variation of this ratio, $]-1, 1/2[$. Indeed, the differential of the strain energy per unit volume is given by $\mathrm{d}w = \varepsilon_{ij}\, d\sigma_{ij} + \theta\, \mathrm{d}p$, and for small strains, the strain energy is quadratic. The restrictions on the coefficients imposed by the nonnegative character of the strain energy are given by $E > 0$, $-1 < \nu < 1/2$, and $Q > 0$, where $1/Q$ stands for the extra amount of relative fluid volume by unit increment of pressure, an amount which can be forced into the structure under pressure while maintaining the overall volume of the structure constant (e.g. see Biot and Willis, 1957). If both phases—structure and fluid—are incompressible, then Q tends to infinity (e.g. see Biot, 1962; Auriault and Sanchez-Palencia, 1977; Naili and Geiger, 1995).

Moreover, a negative drained Poisson's ratio can tentatively be explained by the alveolar interstitial structure. Such structures expand laterally when stretched and contract laterally when compressed. This behaviour is achieved by forming the cells into a "re-entrant" shape which bulges inwards and which unfolds under tension, resulting in a lateral expansion (e.g. see Lakes, 1986, 1987, 1991; Lakes *et al.*, 1988).

The drained Poisson's ratio may greatly alter the overall behaviour of the medium. The consolidation time τ, given by eqn (7), characterizes the speed with which the structure consolidates, i.e. from the very moment after which the transient step effect becomes negligible. Therefore, it is interesting to investigate this effect and the influence of the above parameters on τ, particularly the influence of drained Poisson's ratio. The latter is shown in Fig. 1. It is worth pointing out that τ has the same value—i.e. $\tau \to 0$—in the limits $\nu \to -1$ and $\nu \to 1/2$. In this case, the diffusion equation satisfied by the relative fluid content θ boils down to the Laplace equation because the consolidation constant c tends to infinity while the time variation of the fluid content keeps finite values. In other words, the transient step does not occur for such ν values. On the other part, the consolidation time is shown to be maximal when $\nu = 0$.

Figure 2 shows the force vs time curves during compression and relaxation, given by eqns (15) and (17), for various values of drained Poisson's ratio. In these curves, the duration of compression step t_0 is equal to 40 s; the values of the geometry parameters and the mechanical characteristics have been drawn from the experiment on foam samples as described below. It is interesting to consider the variation of the ordinate at the origin of

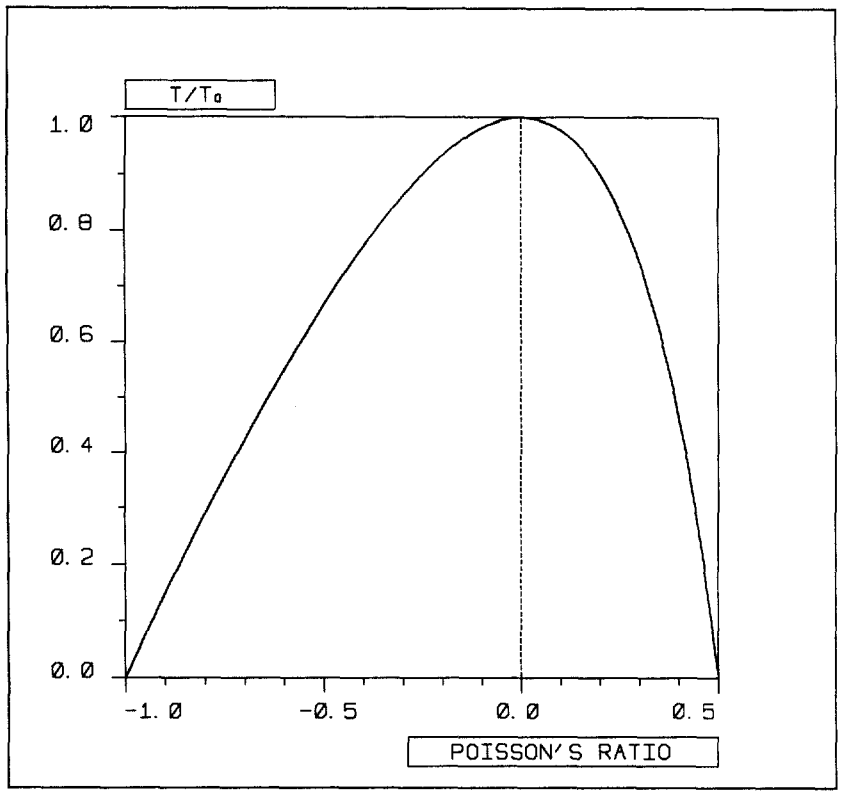

Fig. 1. Characteristic time vs the Poisson's ratio. In this plot, a normalized characteristic time T/T_0 is defined, where $T = \tau$ and $T_0 = a^2\mu/E\kappa$.

$F(t)$ with respect to the drained Poisson's ratio—the latter is shown in Fig. 3. $F(t)$ is found to decrease monotonically in the interval considered above. Since its maximal value for ν tending to -1, corresponds to τ equal to zero, then $F(t)$—as given by eqn (15)—undergoes in this case a sudden upward jump. Likewise, $F(t)$—as expressed by eqn (17)—is subjected, in the same limit, to a downward jump when the relaxation step of the test begins. The explanation of the latter phenomenon is that the speed of filtration becomes infinite. On the contrary, when ν tends to 1/2, both τ and the ordinate at the origin are equal to zero. The function $F(t)$—as expressed both by eqns (15) and (17)—is then equal to its asymptotes in each time interval—compression and relaxation. This may be interpreted as a purely elastic behaviour. In this case, the radial displacement of the solid skeleton has the same velocity as the fluid flow and, consequently, there is simply no filtration.

In addition, if the radius of the cylinder is doubled, the slopes of the curves in the asymptotic behaviour region are in the ratio 1:16, while the ordinate at the origin changes only by a 1:4 ratio. For radial stress vs strain, the slope remains identical for the two radii, while the ordinate at the origin varies by a 1:4 ratio. This clearly shows that the behaviour of the porous medium cannot be described in terms of a Kelvin–Voigt model, for which the characteristic coefficients are not geometry-dependent.

5. EXPERIMENTAL METHOD

5.1. *Rheological tests on the rubber foam*

The rheological tests were performed using a standard tension compression machine. This machine possesses a crosshead whose displacement velocity can be varied and controlled, connected to a recording unit of the signals characterizing both imposed displacement and applied load. The tested foam samples with a discoïdal shape were immersed in water at constant room temperature. Unconfined compression was applied by a circular

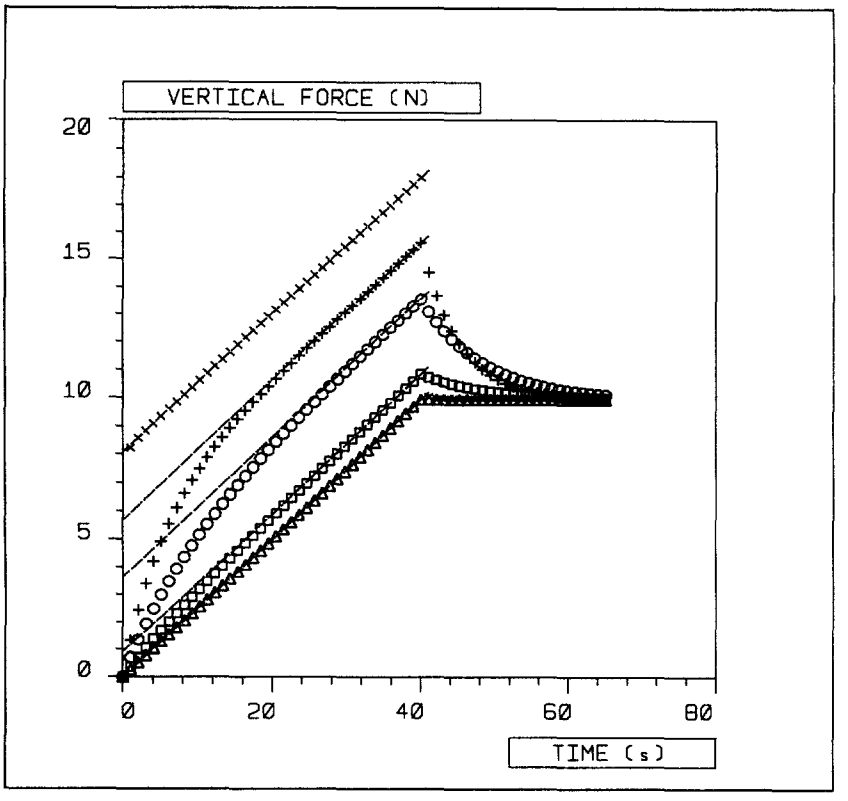

Fig. 2. Evolution with time of the force during compression and relaxation for various values of drained Poisson's ratio. Duration of the compression phase $t_0 = 40$ s. In both cases, the dashed line represents the asymptotic behaviour; drained Poisson's ratio: $\nu = -0.999$ (×), $\nu = -0.75$ (+), $\nu = -0.5$ (○), $\nu = 0$ (□), $\nu = 0.499$ (△).

plate—in polished PMMA of a diameter greater than that of the sample, which was kept rigidly tight to the moving crosshead.

Figure 4 shows the force vs time curve during the compression of the water-saturated rubber foam test sample. The permeability κ of the structure and the dynamic viscosity μ of the fluid were measured, prior to the test. The value of the permeability coefficient, under steady conditions, was obtained by several measurements of the pressure drop-flow rate relationship through the test section of a home-made hydromechanical bench containing the foam material. Using Darcy law:

$$Q_m = \rho \frac{\kappa}{\mu} S_0 \frac{\delta p}{L}$$

where Q_m denotes the mass flow rate measured by weighing, ρ the density of water at the mean temperature of the tests—16°C, L the length of the sample, S_0 the area of the test section and δp the pressure drop measured by a differential transducer, the value of the permeability of the rubber foam was found to be $\kappa = 0.3 \times 10^{-11}$ m^2 and the relative error is estimated at $\pm 3\%$.

Moreover, the fluid saturating the structure was submitted to viscometry tests, using a capillary viscometer which accounts for temperature dependence. The dynamic viscosity of the fluid was found to be $\mu = 1.02 \times 10^{-3}$ Pa s and the relative error is estimated at $\pm 3\%$. Then, the relative error is approximately equal to 5% for ν, if we use eqn (18).

The constituents—rubber foam and water—for this experiment are clearly incompressible. The undrained Poisson's ratio is then equal to 1/2 (e.g. see Duvaut, 1990).

Circles in Fig. 4 represent experimental results obtained during the compression phase. The crosses show the asymptotic behaviour of the force acting on the sample, from which

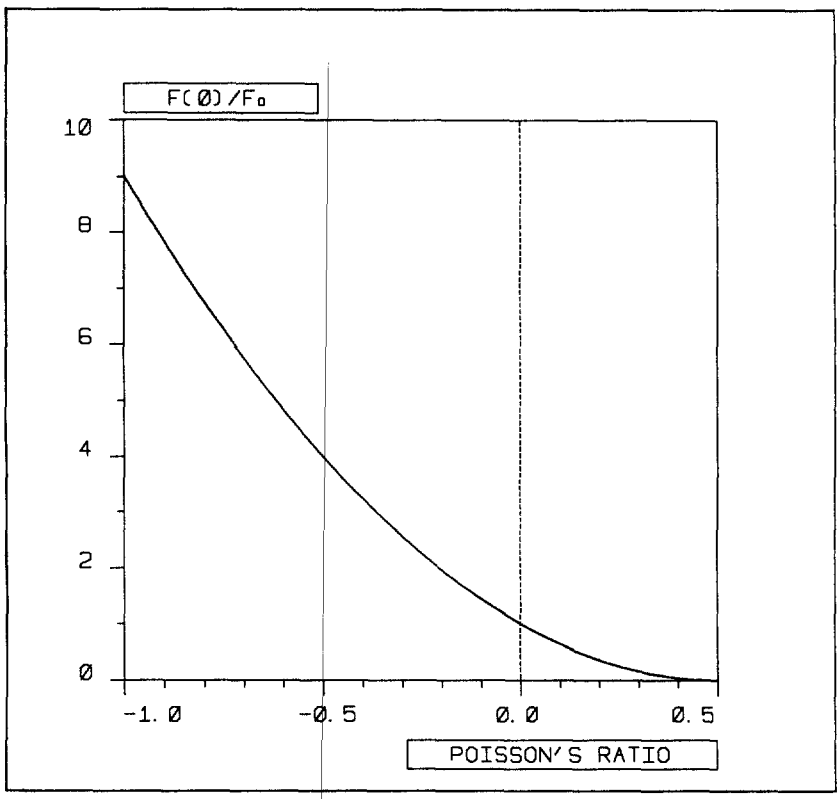

Fig. 3. Effects of the Poisson's ratio values on the ordinate at the origin, for the asymptotic behaviour of the resultant force during the compression phase. In this plot, a normalized force $F(0)/F_0$ is defined, where $F_0 = \pi a^4(v\mu/h8\kappa)$.

the drained Young's modulus and the drained Poisson's ratio of the medium, as described above, are deduced. Hence, we obtained $\nu \sim -0.3$, $E \sim 28{,}500$ N m^{-2} and $\tau \sim 25$ s. The solid line represents the theoretical behaviour obtained by the numerical evaluation of eqn (15), given these experimental values. Thus the suggested methodology can be summarized as follows: in a first step, the load vs time was measured by using the experiment set-up previously mentioned. Then, in a second step, we determine the asymptotic behaviour. Following the method previously described, this asymptote allows the determination of the drained Poisson's ratio and the drained Young's modulus. Lastly, we can use these values in the theoretical model, described by eqn (15), to ensure the validity of the result.

This sufficiently "larger" time presented above will in practice be difficult to specify since the determination of the consolidation time requires an *a priori* knowledge of the material properties that the analysis proposes to determine. Subsequently, it is necessary to run several experiments to obtain one estimation of the parameter values. As shown in Fig. 1, such an order of magnitude of this time $\mu a^2/E\kappa$ is derived from the drained Young's modulus as obtained by measuring the force during the relaxation phase.

Nearly all ordinary materials exhibit a positive Poisson's ratio, i.e. they become smaller in cross-section when stretched and larger when compressed. The permitted range of Poisson's ratio for an isotropic material is $]-1, 1/2[$. The tested foamy materials are produced so that, locally, the ribs protrude inward rather than outward as a "re-entrant" structure. We have visualized stereo photograph of the tested foam showing cells with "re-entrant" shape very similar to the ones given in Friis *et al.* (1988). To visualize the relationship between structure and Poisson's ratio, let us imagine tension to be applied to the vertically protruding ribs. The ribs in the lateral directions will tend to move out, causing lateral expansion. When compression is applied, the ribs, which are already curved inward, will bend further inward, thus resulting in lateral contraction in response to axial compression.

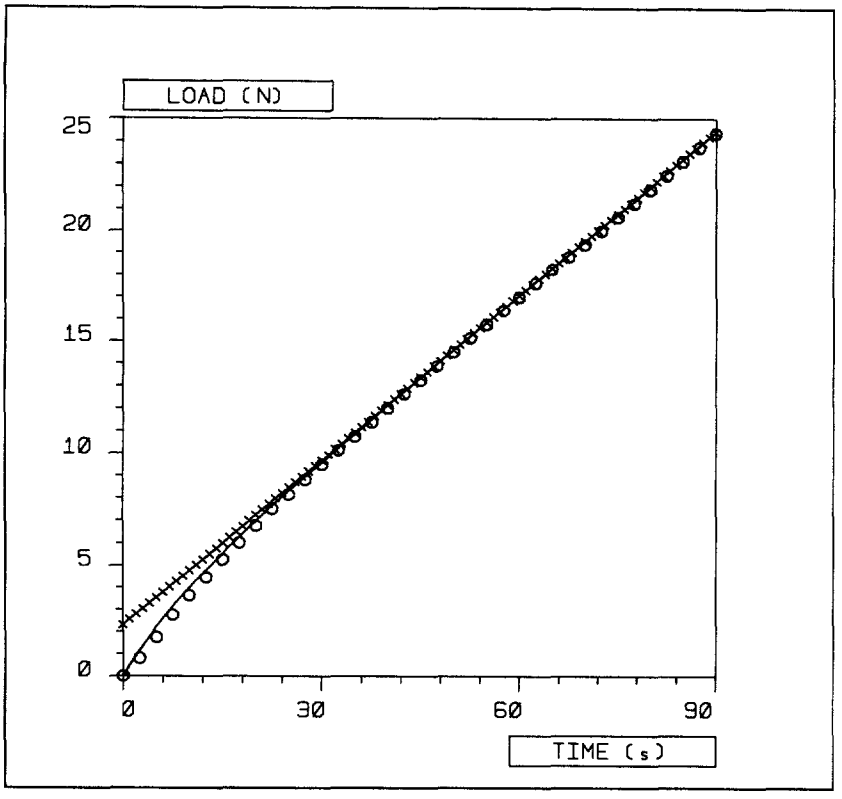

Fig. 4. Force vs time during compression. Foam rubber geometry parameters are: height $h = 30$ mm, radius $a = 50$ mm, and mechanical characteristics $E \sim 28{,}500\ \mathrm{N\,m^{-2}}$, $\nu \sim -0.3$, $\kappa = 0.3 \times 10^{-11}$ $\mathrm{m^2}$; viscosity of water $\mu = 1.02 \times 10^{-3}$ Pa s; crushing rate $v = 3.4 \times 10^{-2}$ mm $\mathrm{s^{-1}}$; duration of compression step $t_0 = 90$ s. Experiment (○), asymptotic behaviour (×), theory (—).

5.2. *Rheological tests on the myocardium tissue in passive state*

An exhaustive understanding of cardiac mechanics and heart pumping performance requires an accurate and complete rheological characterization of myocardial tissue in its passive state. Generally speaking myocardium can be considered as a polyphasic fibrous material whose anisotropic and viscoelastic rheological properties are very complex. Nevertheless, as previously shown in Djerad (1991), when testing the myocardium in passive state, effects of anisotropy both related to elastic properties and water transport permeability proved insignificant. One simple and current way to describe unsteady mechanical behaviour of such biological soft tissue is the well-established Fung's theory of quasi-linear viscoelasticity (e.g. see Fung, 1981). Nevertheless, such a theory does not take into account the microstructural and polyphasic nature of the tested medium as well as considerations related to the porosity and fluid phase effects. Within the framework of Biot's theory of poroelasticity, it is shown here that one has necessarily to take into consideration the motion of the interstitial fluid in order to assess the long-time behaviour of stress relaxation experiments.

Rheological characterization tests under unsteady conditions, controlled temperature and chemical environment, have been performed, using myocardium samples dissected from fresh pig hearts. Although difficult to achieve in the case of such a soft tissue, both a precise geometrical definition and an accurate localization of the sample are needed. Cylindrical core-samples were stamped out from the left ventricle wall; then the extremities were cut out with two parallel blades in order to obtain discoïdal samples whose sides were plane and parallel. According to the localization site, the general orientation of fibres were either perpendicular or parallel to the axis of the sample. These pieces of tissue of different radius—$a = 8$, 11, 18 mm—awash in a physiological solution, were submitted to ramp-relaxation tests under uniaxial unconfined compression, using a home-made test machine.

The deformation was generated by the motion of a solid, waterproof and smooth surface in such a way that the medium was undergoing an increasing strain at constant rate, up to approximately 10% and then was maintained in a constant state of strain. During the ramp phase, a constant strain rate of the order 2.5×10^{-3} s^{-1} was maintained during $t_0 = 40$ s. The Lagrangian stress was recorded for about 1 h typically during such ramp-relaxation tests.

Prior to rheological testing, filtration experiments under steady conditions have been performed with thin discoïdal samples of 20 mm diameter and 2 mm height. Although experimental data were relatively sparse, due to both differences in sampling sites, states of tissue preservation and obvious nonlinear behaviour of filtration processes at high pressure gradients, they did not reveal any marked anisotropic effects. Referring to these data (see Djerad, 1991; Djerad *et al.*, 1992, Oddou *et al.*, 1993), an approximate value of 10^{-15} m^2 has been chosen for the permeability coefficient of such a myocardial tissue.

One important outcome of poroelasticity phenomena is the fact that the resulting stress relaxation process has a characteristic time, depending upon the size of the tested medium—as related by eqn (7). All parameters—other than the radius—being maintained constant, the slope of the time evolution of the stress at the beginning of the relaxation process depends upon the sample size (see Fig. 5). From measurements obtained with samples of different sizes, the characteristic times have been deduced. These experimental data, as reported on Table 1, are clearly showing that the consolidation time is proportional to the square of the sample radius, as inferred from the present theory of poroelasticity.

The theoretical relations, given by eqns (14) and (16), yielding stresses evolution as a function of time are written as a series of exponentials, highlighting the characteristic time τ. All the parameters have been independently measured except for the Poisson coefficient

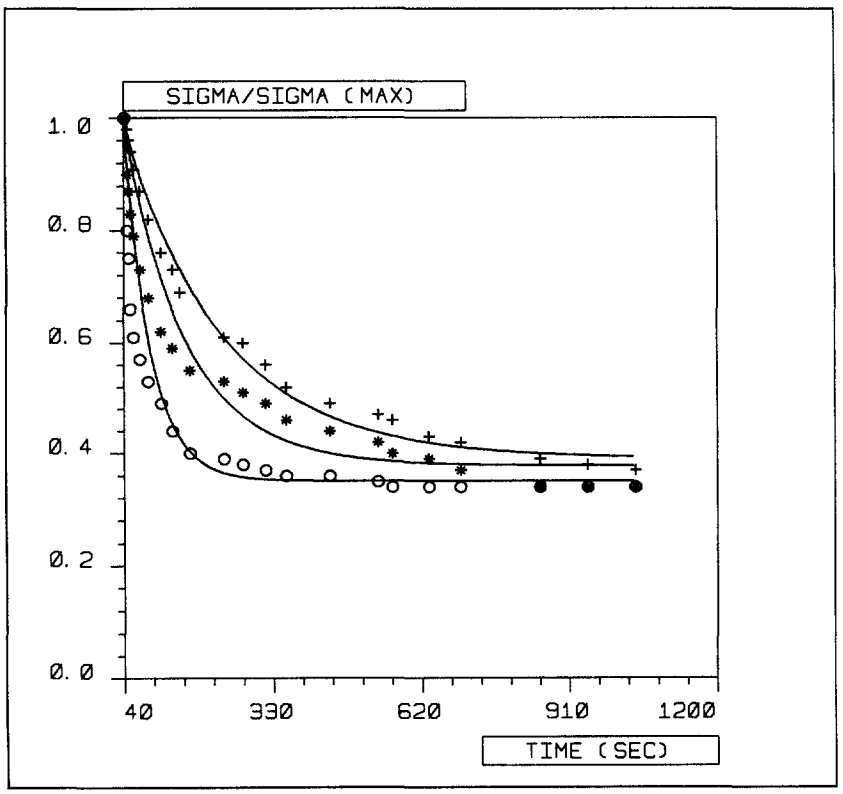

Fig. 5. Experimental and theoretical data concerning temporal evolution, during the relaxation phase, of normalized axial stress—instantaneous value of stress divided by is maximal value at $t_0 = 40$ s—for three myocardium samples with a different radii. Experimental and numerical data from poroelasticity $E = 4100$ N m^{-2}, $\mu = 1.02 \times 10^{-3}$ Pa s, $\nu = -0.15$, $\kappa = 10^{-15}$ m^2, $h = 10$ mm. Radius: $a = 8$ mm (○), $a = 11$ mm (*), $a = 18$ mm (+).

Table 1. Characteristic times of relaxation as experimentally obtained for three discoïdal samples with different radii. Note the proportionality of these times with the square of the characteristic lengths, radii, of the samples

a (mm)	τ (s)	τ/a^2 (s m^{-2})
8	26	0.406×10^6
11	47	0.388×10^6
18	135	0.416×10^6

which could not be assessed. So as to obtain the best possible model compared to the experimental results, a negative value of the Poisson ratio had to be chosen. To this end, we use the least-squares method. A negative value of ν emphasizes the transverse shrinkage of the matrix under a compression load. This type of behaviour may be due to the architecture of the tissue, giving rise to "re-entering alveola" (e.g. see Lakes, 1986, 1987, 1991). Figure 6 puts in evidence the near-perfect match between our experimental data and the theoretical results over the overall ramp-relaxation process.

It is worth noting that the unsteady and passive rheological behaviour of most biological materials has been viewed, thus far, along the quasi-linear viscoelasticity model; such a model, indeed, accounts for the linear decrease of the reduced relaxation $G_r(t)$—stress normalized by its maximal value—in terms of the logarithmic function of time, over three decades at least. Such a phenomenon, which has been observed in our data for a short duration of the ramp phase—duration 0.35 s, maximal strain amplitude 10%—is well correlated, for the long times, with the poroelasticity theory (see Fig. 7). Nevertheless, the sole poroelasticity model was unable to give a full account of the relaxation spectrum; particularly, it is wondered whether intrinsic viscoelastic properties of the fibrous matrix as well as the intracellular medium play a significant role for the short times.

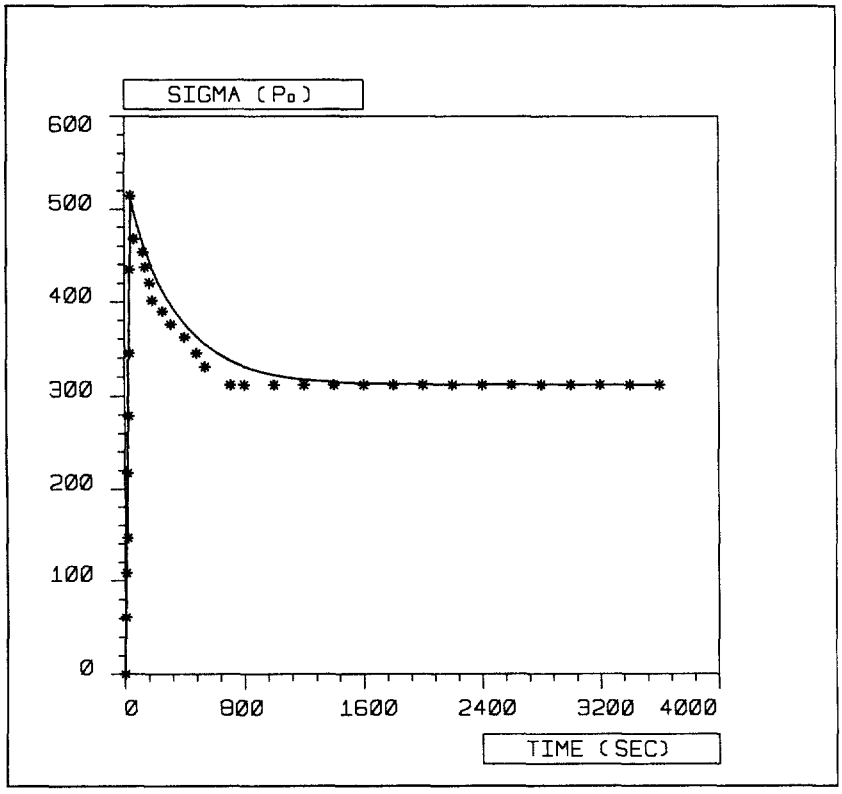

Fig. 6. Time variation of the stress in a ramp–relaxation compression test: experimental (*) and numerical (—) data from poroelasticity theory. The same parameters as in Fig. 5 with $a = 11$ mm.

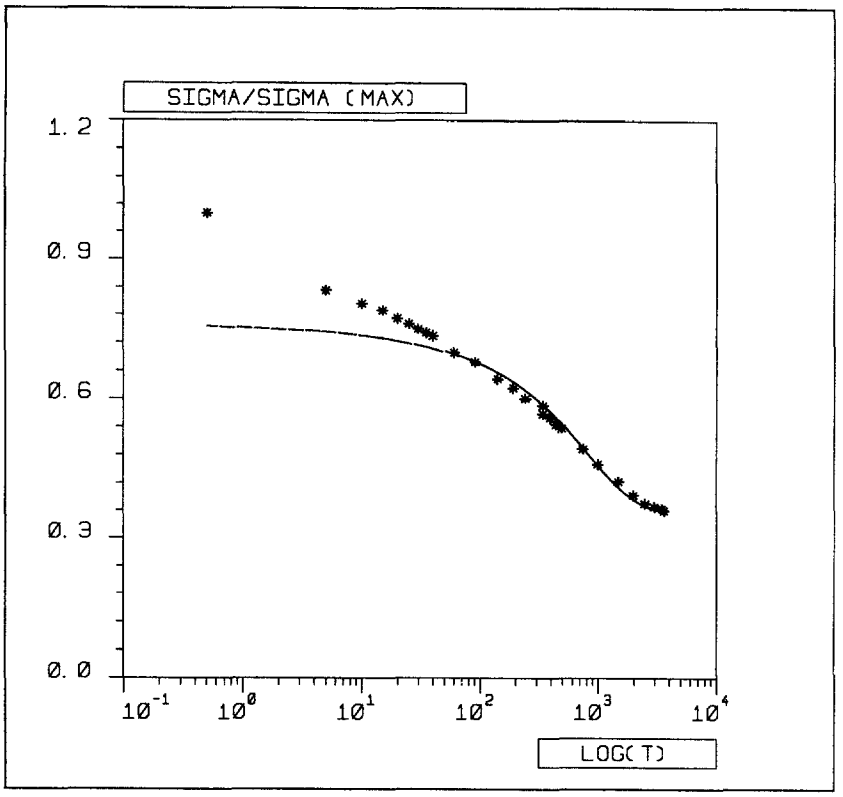

Fig. 7. Time variation of reduced stress relaxation function for a compression test with a very short time of loading. The same parameters as in Fig. 6 with $t_0 = 0.35$ s. Experimental data (*), poroelasticity theoretical data (—).

Such a viewpoint concerning the unsteady rheological behaviour at long times of myocardial tissue has to be confirmed by further rheological experiments with different means of solicitations and boundary conditions. As has been done here, it will be worth re-examining the data derived from other biological soft tissues—e.g. vascular wall, ligaments. Most interpretations, based, so far, upon the viscoelasticity theory alone, would be likely to conform with a more physical framework thanks to what has just been developed with concepts using the poroelasticity theory.

5.3. *Rheological tests on the fibroblastic biological collagenic gels*

The human skin is a barrier organ that performs many essential functions, first by limiting water loss and thus contributing to fluid and temperature homeostasis, and also by protecting against physical, chemical and microbiological aggression. It consists in three basic components: keratinocytes, fibroblasts and collagen. Various skin culture models have been developed for years, not only for wound covering but also for studying the intrinsic physiology and cutaneous pharmacology.

The mechanical interactions between the fibroblasts and the extracellular collagenic matrix play an important role in the interpretation of the rheological behaviour of a dermis equivalent during its construction phase which only last a few days. In these interactions, the key phenomenon is the local traction force exerted by cells on the collagen network in extracellular matrix, which results in a compaction of the medium as well as a mechanical integrity of the tissue. The diameter reduction rate of gels is very dependent on the rheological properties of fibroblast-populated collagen gel. Reconstructed dermis equivalent can be considered as a biphasic poroelastic medium. The determination of unsteady rheological tissue properties during the relaxation test, under unconfined compression, should give us more information about this biological gel with respect to its microstructural evolution.

The biological gel was obtained by the association of two essential components: fibroblasts and collagen. For a 60 mm diameter bacteriologic Petri dish, the culture was prepared with 2.3 ml of concentrated culture medium, 0.45 ml of serum, 1–3 ml of collagen in solution, 0.25 ml of 0.1 N NaOH and 3 ml of fibroblast suspension—3×10^5 cells/ml—in a culture medium with serum. The mixture polymerized rapidly when placed in an incubator at 37°C and pH 7.4, under a humid atmosphere with 5% CO_2. Initially, the fibroblasts, uniformly dispersed throughout the collagen gel, were interacting with collagen; the sample being compacted in a period of time of about 10 days (e.g. see Oddou *et al.*, 1995).

When compacted and sufficiently rigid, the samples were tested using the same rheological methodology as previously described, involving here a series of ramp-relaxation compressive increasing strains. Such unconfined and uniaxial compression was induced by the relative displacement of a piston with a constant velocity during a short period of time, ~ 1 s, followed by a long pause, $\sim 1.5 \times 10^3$ s. The displacement was created by a step motor driven by a computer. The resulting response of the compression force acting upon the gel was measured by means of a force captor. The tests were carried out at room temperature and the gel sample kept inside a physiological culture solution during the overall experiment. We have taken into account the influence of the parasitic. Archimède force on the data worth measuring. For each step of increased deformation, we were particularly interested in both maximal forces at the end of the ramp phase and relaxed minimal forces at the end of the step. The experimental data were then recorded and analyzed in terms of Lagrangian stresses.

The experimental results, as presented in Fig. 8, emphasize the pseudo stress–strain relationships of the biological gels both for unsteady maximal stresses—recorded after each end of the ramp phase—and relaxed minimal stresses at the end of the relaxation phase. It

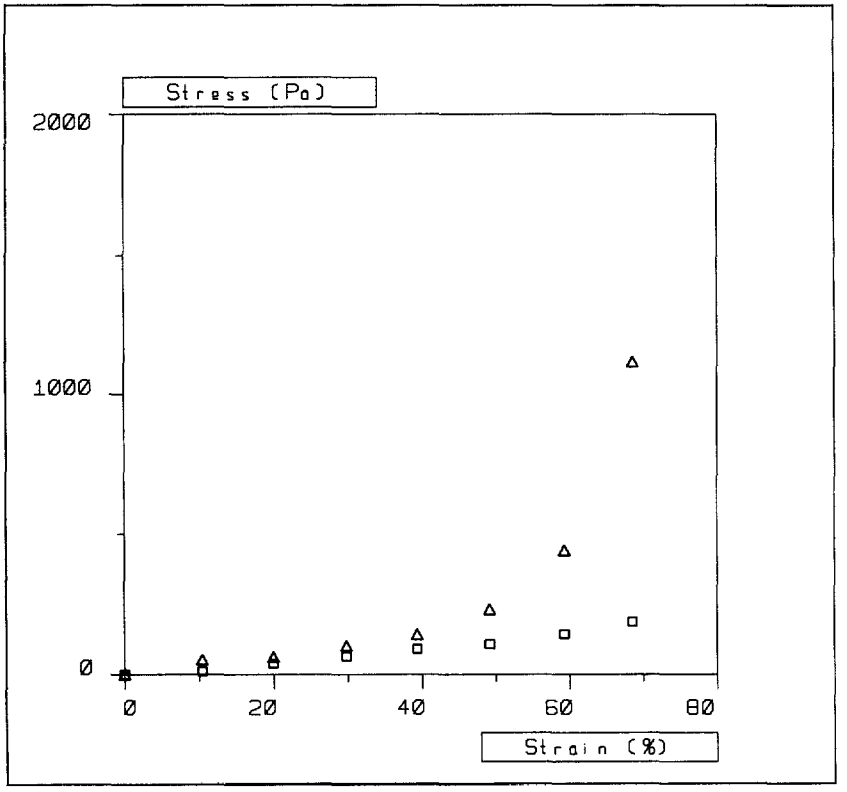

Fig. 8. Stress–strain relationships as experimentally obtained with a biological gel tested by a series of increased ramp–relaxation unconfined compression steps. Short-time response (△), relaxed response (□)—see text for details in the experimental protocol.

can be noted that the former is a nonlinear and increasing function while the latter reveals to be quasi-linear.

The maximal stresses recorded for a "short time" being a manifestation of the fluid movement while the relaxed stresses represent the static elastic behaviour of gels, it is suggested that this nonlinear behaviour is principally due to the properties of the matrix permeability, under increased compression. This phenomenon may involve fluid movements inside the gels as well as the structure of the collagenic matrix. When the gels are compressed, interstitial fluid inside the media are subjected to a three-dimensional stress field. The induced motion of the fluid then leads to a change in the architecture of the collagen fibrils network. Varying with the direction of the solid local structure displacement and fluid relative velocity, the collagen fibrils rearrange in both longitudinal and azimuthal directions: some fibrils are compressed in the vertical direction while others are stretched in the azimuthal one. Under such an unconfined and unsteady compression test, the local mechanical properties show an anisotropic unsteady elastic behaviour, which can be represented by a smaller elasticity modulus in vertical direction than the one in azimuthal direction. The latter effect associated with the fluid action may explain why the peak forces, after each impulse, increase in a nonlinear way, due to both non-linearity in permeability and elasticity in collagenic fibrils extension.

So, a fibroblast-populated collagen gel is a complex tissue-like medium that requires a thorough rheological characterization. The local phenomena we have just described above, result in relaxation processes where the reduced stress relaxation function, as illustrated in Fig. 9, depends upon the initial state of strain. These experimental results show that the medium does not behave as a quasi-linear viscoelastic tissue but has to be roughly modelized by a standard Kelvin–Voigt solid with a nonlinear damper and spring. Nevertheless, the fact that the characteristic time damping does not significantly vary in function of the

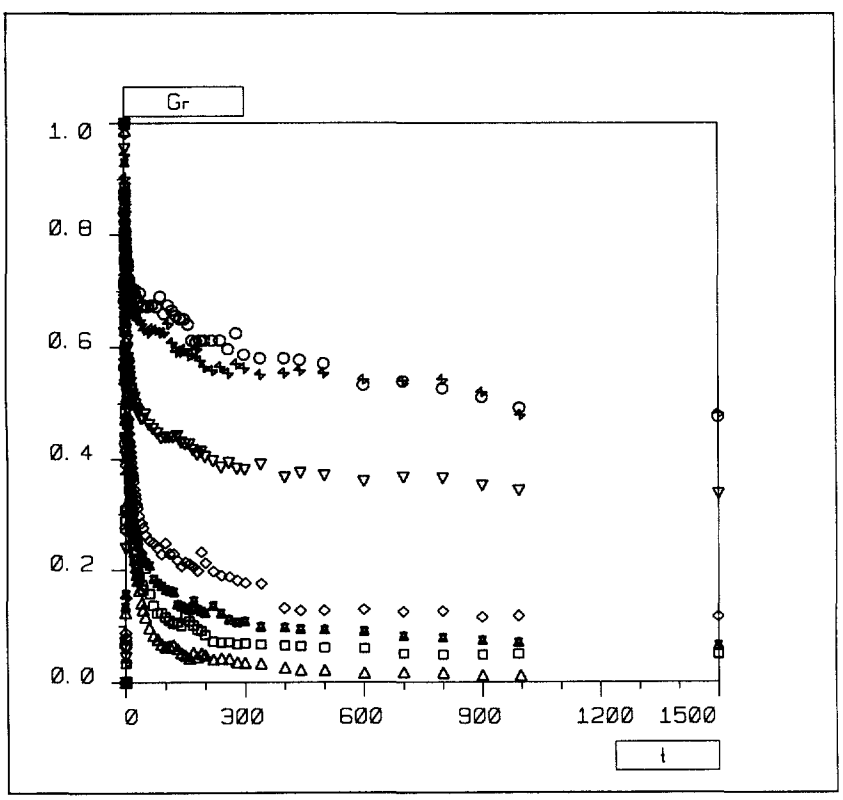

Fig. 9. Time-variation of reduced stress–relaxation function for a biological gel in unsteady and unconfined compression tests. The same protocol as in Fig. 8. Strain: 10% (○), 20% (▷◁), 30% (▽), 40% (◇), 50% (✡), 60% (□), 70% (△).

deformation and that the effects of fibroblast cells are time-dependent at the time scale of the experiment, remains actually unclear.

6. CONCLUSION

This work proposes both the determination of drained Young's modulus, and drained Poisson's ratio of a porous deformable medium, saturated by a Newtonian fluid under a constant rate unconfined compression test of a cylindrical sample, using the measured axial force variation with time. The suggested method for determining the drained Poisson's ratio takes advantage of the transition state from undrained to drained response, that takes place if the duration of the test is long enough compared to the characteristic time. For a constant rate of axial deformation, this transition state is reflected by a continuous decrease with time of the changing rate of the axial force from the undrained to the drained value. The proposed method for determining drained Poisson's ratio is based on the interpretation of the y-intercept of the line characterizing the drained response, in a plot of the axial force vs time. However, for a very long consolidation time, this approach may be unsuitable if it is not possible to adjust the strain rate for maintaining the small strains hypothesis.

For future developments of this method as applied to living soft tissues, the case where both phases are compressible can be of interest. Under such a circumstance, there are six mechanical parameters—drained Young's modulus, undrained and drained Poisson's ratio, "induced pore pressure coefficient", permeability of the structure, and the dynamic viscosity of the interstitial fluid—in the model describing the mechanical behaviour of the porous elastically deformable medium. The basic idea of our method is to take advantage of the asymptotic behaviour in a unconfined compression relaxation test. This idea is further valid in the case where the constituents are compressible for determining the drained Young's modulus and the drained Poisson's ratio. Indeed, it is easy to see that the problem of the compression of the porous elastically deformable medium becomes, when formulated in terms of velocity, formally analogous to a classical problem of the elasticity of a deformable medium under compression, for times longer than the consolidation time τ.

Acknowledgement—The authors are gratefully indebted to Dr B. Coulomb and his team, from the "Laboratoire de Dermatologie, INSERM U 312, Hôpital Saint-Louis, Paris" for providing the derm gels and related helpful suggestions concerning biological viewpoints.

REFERENCES

Armstrong, C. G., Lai, W. M. and Mow, V. C. (1984) An analysis of the unconfined compression of articular cartilage. *Journal of Biomechanical Engineering, ASME* **106,** 165–173.

Auriault, J.-L. and Sanchez-Palencia, E. (1977) Étude du comportement macroscopique d'un milieu poreux saturé déformable. *Journal de Mécanique* **16**(4), 577–603.

Biot, M. A. (1941) General theory of three dimensional consolidation. *Journal of Applied Physics* **12,** 155–165.

Biot, M. A. (1946) Theory of propagation of elastic waves in a fluid saturated porous solid, Parts I and II. *Journal of the Acoustical Society of America* **28**(2), 168–191.

Biot, M. A. (1962) Mechanics of deformation and acoustic propagation in porous media. *Journal of Applied Physics* **34**(4), 1482–1498.

Biot, M. A. and Willis, D. G. (1957) The elastic coefficients of the theory of consolidation. *Journal of Applied Mechanics, ASME* **24,** 594–601.

Bourbié, T., Coussy, O. and Zinszner, B. (1987) *Acoustics of Porous Media.* Éditions Technip.

Coussy, O. (1991) *Mécanique des Milieux Poreux.* Éditions Technip.

Djerad, S. (1991) Rheological characterization of fibrous and polyphasic materials. Applications to cardiac muscle tissue (in French). Ph.D. thesis, University Paris XII.

Djerad, S., Du Burck, F., Naili, S. and Oddou, C. (1992) Analysis of the unsteady rheological behaviour of a sample from cardiac muscle. *C.R. Acad. Sci. Paris* **315,** Série II, 1615–1621.

Duvaut, G. (1990) *Mécanique des Milieux Continus.* Masson.

Friis, E. A., Lakes, R. S. and Park, J. B. (1988) Negative Poisson's ratio polymeric and metallic foams. *Journal of Materials Science* **23,** 4406–4414.

Fung, Y. C. (1981) *Biomechanics: Mechanical Properties of Living Tissues.* Springer-Verlag.

Kim, Y.-J., Bonassar, L. J. and Grodzinsky, A. J. (1995) The role of cartilage streaming potential, fluid flow and pressure in the stimulation of chondrocyte biosynthesis during dynamic compression. *Journal of Biomechanics* **28**(9), 1055–1066.

Lakes, R. (1986) Experimental microelasticity of two porous solids. *International Journal of Solids and Structures* **22,** 55–63.

Lakes, R. (1987) Foam structures with a negative Poisson's ratio. *Science* **235,** 1038–1040.

Lakes, R. (1991) Deformation mechanics in negative Poisson's ratio materials: structural aspects. *Journal of Materials Science* **26,** 2287–2292.

Le Gallo, O., Naili, S. and Geiger, D. (1991) Caractérisation d'une structure poroélastique par un essai de compression. *Résumé des Communications du* 10e Congrès Français de Mécanique, Paris, 2–6 Septembre, Tome **1,** 329–332.

Mak, A. F. (1986) Unconfined compression of hydrated viscoelastic tissues: a biphasic poroviscoelastic analysis. *Biorheology* **23,** 371–383.

Mandel, J. (1953) Étude mathématique de la consolidation des sols. *Geotechnique* **3,** 287–299.

Mow, V. C., Kuei, S. C., Lai, W. M. and Armstrong, C. G. (1980) Biphasic creep and stress relaxation of cartilage in compression: theory and experiments. *Journal of Biomechanical Engineering* **102,** 73–84.

Mow, V. C., Kwan, M. K., Lai, W. M. and Holmes, M. H. (1986) A finite deformation theory for nonlinearly permeable soft hydrated biological tissues. In *Frontiers in Biomechanics*, ed. by G. W. Schmid-Schönbein, S. L.-Y. Woo and B. W. Zwiefach, pp. 153–179. Springer-Verlag.

Naili, S. and Geiger, D. (1995) Some remarks about the mechanics of porous elastically deformable media. *Applied Mechanics Reviews, ASME* **48**(10), 707–716.

Naili, S., Le Gallo, O. and Geiger, D. (1992) Characterization of a porous elastically deformable medium by a compression–relaxation test. *C.R. Acad. Sci. Paris* **315,** Série II, 1439–1444.

Naili, S., Le Gallo, O. and Geiger, D. (1994) Identification of mechanical parameters in a porous elastically deformable medium by a compression–relaxation test. *Journal of Applied Mechanics, ASME* **61,** 985–988.

Oddou, C., Li, F. and Coulomb, B. (1995) Role of cells in the unsteady mechanical behavior of biological gels. Mini-symposium on biorheology in cellular interaction and tissue engineering. Abstracts of the 9th International Congress of Biorheology, Big Sky, Montana USA. *Biorheology* **32**(2–3), 197.

Oddou, C., Naili, S., Du Burck, F. and Djerad, S. (1993) Unsteady rheology and poroelasticity of myocardial tissue. Bioengineering Conference ASME, 25–29 June 1993, Colorado (USA), ed. N. A. Langrana, M. H. Fiedman and E. S. Good. *BED* **24,** 52–55.

Rice, J. R. and Cleary, M. P. (1976) Some basic diffusion solutions for fluid-saturated elastic porous media with compressible constituents. *Reviews of Geophysics and Space Physics* **14**(2), 227–241.

Spilker, R. L., Suh, J.-K. and Mow, V. C. (1990) Effects of friction on the response of articular cartilage: a finite element analysis. *Journal of Biomechanical Engineering, ASME* **112,** 138–146.

Yang, M. and Taber, L. A. (1991) The possible role of poroelasticity in the apparent viscoelastic behaviour of passive cardiac muscle. *Journal of Biomechanics* **24**(7), 587–597.